DOI: https://doi.org/10.53555/nnas.v8i1.1237 Publication URL: https://nnpub.org/index.php/AS/article/view/1237

PARAMETRIC ANALYSIS AND OPTIMIZATION OF AL-MG-SI/EGGSHELL PARTICULATE COMPOSITE MATERIAL USING RESPONSE SURFACE METHODOLOGY

S.C Eze[1*], D.S Yawas[2], E.T Dauda[3] and C.O Izelu[4]

*[*1]PG Student, Mechanical Engineering Department, FOE, ABU, Zaria, Kaduna State Nigeria*
[2]Professor, Mechanical Engineering Department, FOE, ABU, Zaria Kaduna State Nigeria
[3]Professor, Metallurgical and Materials Engineering Department, FOE, ABU, Zaria Kaduna State Nigeria
[4]Professor, Mechanical Engineering Department, COT, FUPRE Effurum, Delta State, Nigeria

*[*1]samchikeze@gmail.com and samezeng@yahoo.com, [2]dyawas@yahoo.com*
[3]emmayustoi@yahoo.com and emmadaudayusuf@gmail.com, [4]izelu2003@yahoo.com and izelu.christopher@fupre.edu.ng

Corresponding Author: -
samchikeze@gmail.com

Abstract- *In this study, Al-Mg-Si alloy obtained from scrap aluminum profile was reinforced with calcined eggshell particulates at varying particle sizes (25µm, 50 µm and 75 µm) and concentrations (1wt%, 2 wt% and 3 wt %) respectively. Data generated from series of experimental runs in which the effect of the factor inputs such as eggshell size and concentration had on the response variables (hardness, yield strength, modulus of elasticity, thermal conductivity, impact strength, density and corrosion rate) of the Al-Mg-Si/Eggshell particulate composite material were recorded The response surface methodology, based on central composite design of experiment, was used and the analysis performed in Design Expert 9 software environment. Regression models were obtained and evaluated for the response variables as functions of the selected factors. The optimal settings of these factors required to either maximize or minimize the response variables were also determined. The result showed that the optimum setting of the factors 'A' (ESP size) at 25 µm, and 'B' (ESP Conc.) at 1wt. %, would maximize H to a value of 34.876 BHN, YS to a value of 38.163 N/mm^2, ME to a value of 23729.405 N/mm^2 TC to 54.672 W/m.^{o}C, and IE to 15.218 J while minimizing D to a value of 2623.058 Kg/m^3 and CR to a value of 0.921 MPY respectively with desirability of 0.940332, 0.363653, 1.00, 0.516979, 0.519945, 0.37036 and 0.916263 which occurred within the selected design space.*

Keywords- *Al-Mg-Si alloy, scrap aluminum profiles, eggshell particulates, response surface methodology, Design Expert software*

I.INTRODUCTION

Most composites consist of a bulk material (the 'matrix'), and a reinforcement of some kind, added primarily to increase the strength and stiffness of the matrix. The findings of [1], and [2] confirmed that aluminum-silicon (AI-Si) alloys as matrix are most versatile materials used in the production of aluminum cast parts for the automotive industry. The attraction of aluminium alloys and its composites is also supported by the fact that the required alloy matrix can be obtained at a lower cost through secondary production route of recycling discarded aluminium products such as profiles. Previous studies by [3] revealed that there is no difference in quality between virgin and recycled aluminium alloys.. According to [4], [5] and [6], an added advantage of the use of aluminium scraps for the production of aluminium alloys/composites for engineering applications is in the great amount of energy savings and reduction in the greenhouse gas emissions peculiar to primary aluminium production from the ore. Results from their studies revealed that the properties of the product alloys/composites are comparable with those from primary aluminium The choice of eggshells as reinforcement is mainly because of its low cost and availability. The study by [7] showed that eggshells are available as waste materials and can be obtained from hatcheries, homes and fast food industries They can also be easily collected in good quantities The use of eggshell as reinforcement is supported by the works of [8], [9], [10],[11],[12], [13],[14] and[15].They all reported improvement in a wide range of property values with eggshell particle reinforcement. The quality of composite material suitable for use in automotive parts production depends largely on its capacity to withstand external influences such as load and environmental conditions. These performance requirements are basically determined by using appropriate standard procedures and process techniques that would help to achieve desirable factor mix .An optimization process by considering multiple responses simultaneously is called Multi-response optimization. This is often done to meet with demands of customers on quality, compatibility reliability and functionality. A wide range of multi-response optimization techniques, also sometimes called multi-criteria decision making (MCDM) techniques, have been investigated by varied scholars. In the reviewed works of [16], [17], techniques like finite element, fuzzy logic, genetic algorithm, scatter search, Taguchi, response surface and artificial neural network have been highlighted as process optimization techniques. Relevant to these are works of [18, 19],[20],[21],[22],[23].[24] and [25].

II. MATERIALS AND METHODS

A. Materials

Materials used in this study were **c**hicken eggshells obtained from Food Delight Bakery (a restaurant) located at Sabon Tasha district of Kaduna, Kaduna State of Nigeria and the aluminium profile scraps sourced from a local fabricator (Unique Fabrication of Plot 459 Kachia Road) here in Kaduna, Kaduna State of Nigeria. Both are shown in Figures 1and 2 respectively.

Figure 1. Chicken Eggshell,

Figure 2 Scraps of Aluminum Profile

B. Methods

1 Processing of Eggshells

Five (5) kg of eggshells were rinsed in water to remove the dirt and then packed in a circular stainless steel tray. The rinsed eggshells contained in the tray were dried in the sun for 6 hours. The dried eggshells were crushed as in Figure 3 with the aid of a gyratory crusher. The crushed eggshells from the crusher were later pulverized in a planetary ball mill and offloaded. The pulverized ESP was subjected to XRF examination before calcinations at optimum conditions of 900^{o}C and 2.5hrs. The calcined eggshell powder with CaO yield of 99.6 wt% was sieved into different sizes using sieves of different mesh sizes that ranged from 25 to 125 µm as shown in Figure 4. in accordance with BSI377: 1990 standard as reported by [26].

Figure 3. Crushed Eggshells

Figure 4 Sieved Sizes of Calcined Particulates

2. Processing of Scrap Aluminum Profiles

Seventy-Five (75) kg of scrap aluminum profiles were packed into a crucible and heated in a coal fired furnace to750^{0}C. Thereafter, the crucible containing the melt was removed from the furnace where the slag floating on top (due to plated paint, oxides and scale surfaces around the profiles) were skinned off the surface of the melt. The melt in the crucible was returned to the furnace and then re-heated to 730^{0}C as the optimum pouring temperature for aluminum alloy. Processing was done according to the method suggested by [27]. The operating temperatures were monitored using highly sensitive Optical pyrometer. Finally, the melt (Al-Mg-Si alloy) was cast into 2.5kg aluminum bars as samples/specimen for further development

3. Experimental Set-up for Composite Blending

The processed Al-Mg–Si alloy matrix and eggshell particulate reinforcement were blended out using the stir – casting method. A factorial design was chosen, so that different interactions between independent/input and output variables could be effectively investigated. The relevant input variables in this study were ESP size (A) and ESP concentration (B) as set out in Table 1 A total of nine (9) new samples were produced from the experimental runs with varying eggshell particle sizes of 25, 50, 75µm and concentrations of 1%, 2% and 3% respectively. A control sample without ESP addition was also produced

The output or response variable**s** consisted of performance factors considered fundamental to the development of a suitable composite. These are hardness (H), yield strength YS), modulus of elasticity (ME), thermal conductivity (TC), density (D),corrosion rate (CR) and impact energy (IE).The hardness value of the samples were determined according to ASTM E18 – 79(2000) using Karl Frank Rockwell hardness tester (model 38506). The yield strength and modulus of elasticity values were obtained from tensile tests which were determined according to ASTM D2000 by using the Testometric tensile testing machine, Model FS300AT. The thermal conductivity test was carried out in accordance with the Lee's Disc Method. Impact Strengths were conducted using a fully instrumented Avery Denison Notch Bar impact testing machine according to ASTM D, 2000 standard. The densities of the samples were obtained by using the basic method of determining the density of a specimen by measuring the mass and volume of the specimen and applying relationship: Density = mass/volume (g/cm^{3}) The standard immersion corrosion test was used to investigate the weight

loss and corrosion rates of the specimen in specified electrolytes. The weight loss was determined by finding the difference between the initial weight of the coupon and the final weight after twenty (20) days.

4. Parametric Analysis and Optimization

The response surface methodology (RSM), based on central composite (CC) design of experiment (DOE), was used in this work to model, predict and optimize *Hi, YSi, MEi, TCi, IEi,Di* and *CRi* as a functions of A and B. It is a technique employed for treatment of problems involving a response of interest as a function of several variables according to [28]. The central composite (CC) was selected for the design of the experimental runs. Analysis of variance (ANOVA) was used to validate the developed models, and also, to predict the effect of selected factors A and B on the responses. These activities were carried out in the Design Expert 9 software version 9.0 6.2 environment.

III.RESULTS AND DISCUSSION

A. Chemical Composition of Eggshell Particulates

TABLE 1: CHEMICAL COMPOSITION OF EGGSHELL PARTICULATES

Element	Al_2O_3	CaO	Fe_2CO_3	CuO	As_2CO_3	SrO	RuO_2	Ag_2O	CeO_2	ErO_2	Yb_2O_3	Ta_2O_6	PbO
Composition (wt. %)	2.000	95.180	0.120	0.006	0.120	0.559	0.340	1.400	0.053	0.006	0.003	0.010	0.170

XRF analysis of eggshell particulates (ESP) of Table 1 showed that CaO and Al_2O_3 were the major constituents of uncalcined eggshell accounting for 95 and 2 wt. % respectively. This is in agreement with the findings of [9][10][16] and [18]. The presence of hard compounds like Fe_2O_3 and CuO suggests that eggshell can be used as particulate material for reinforcement.

B. Chemical Composition of Scrap Aluminum Profile

TABLE 2: XRF RESULT OF SCRAP ALUMINUM PROFILES

Element	Mg	Al	Si	S	Ca	Ti	Cr	Mn	Fe	Cu	Zn	Sn	Ba	Pb	Total
Composition (wt. %)	7.617	79.210	12.623	0.081	0.060	0.017	0.004	0.019	0.270	0.030	0.046	0.002	0.017	0.004	100.00

From Table 2, XRF analysis confirmed that aluminum profile scrap examined had as its major constituents: aluminum (Al), magnesium (Mg) and silicon (Si). The three (3) elements alone constituted 99.45% by weight of the aluminum profile sample. The aluminum alloys of the 6xxx series contain an excess of Si above that required to form stoichiometric Mg_2Si. The presence of excess Si changes the composition and density of metastable β″ particles. This finding supports the classification of aluminum profile as a member of Al-Mg-Si alloys family. The presence of other trace elements like zinc (Zn), iron (Fe) and copper (Cu) may have contributed to the enhancement of various mechanical properties as reported by [29] reveals that Cu and Mg improve the mechanical properties of strength at room and elevated temperatures and also make the alloy responsive to heat treatment. The acceptability of high silicon content in this matrix samples is support by [1], that the castability of the composite is enhanced by the high presence of silicon which improves the fluidity of the molten composite and enables it to exhibit excellent dimensional stability, surface hardness and wear resistant properties.

C. Test Result of Properties of Al-Mg-Si/ESP Composite

Properties of Al-Mg-Si matrix and Al-Mg-Si/ESP composite investigated are hardness (H), yield strength (YS), modulus of elasticity (ME), thermal conductivity (TC), density (D), corrosion rate (CR) and impact energy (IE). The results are as presented in Table 3

TABLE 3: TEST RESULT OF PROPERTIES OF AL-MG-SI/ESP COMPOSITE

Exp. Run	Response (Properties)						
	H (HRB)	YS (N/mm^3)	ME (N/mm^3)	TC (W/mk)	IE (J)	D (Kgm^{-3})	CR (MPY)
R_0	30.0	42.235	7,208	83.88	25.00	2748	0.000
R_1	32.0	44.394	15,941	89.96	19.50	2624	0.000
R_2	33.0	59.673	25,938	91.71	13.25	2616	0.000
R_3	36.3	68.054	38,376	101.28	13.00	2529	9.905
R_4	30.7	29.413	12,083	86.93	15.00	2662	0.000
R_5	31.3	35.158	16,623	89.35	20.50	2595	16.671
R_6	36.3	48.480	02,278	90.23	13.50	2569	0.000
R_7	32.8	51.325	10,935	86.62	15.00	2649	3.488
R_8	33.7	44.838	23728	95.38	13.50	2624	0.000
R_9	35.0	29.570	32,347	112.23	09.50	2618	0.000

It was observed that a considerable improvement in the mechanical properties of Al-Mg-Si/ESP composite relative to Al-Mg-Si (scrap aluminium profiles) was achieved. This can only be attributable to the addition of eggshell particles as reinforcement. There were substantial increases in the values of hardness, yield strength, elasticity and thermal conductivity of the un-reinforced alloy from 30BHN, 42.235 Nmm^2, 7208 Nmm^2 and 83.88 W/mk respectively up to maximum values of 36.3HRB, 68.054 Nmm^2 38,376 Nmm^2 and 112.23 W/mk respectively. However, it was accompanied by a reduction in impact strength, density and corrosion rate from raw values of 25J, 2748 $kg/m^3$and 0 mpy respectively down to 9.5J, 2529 $kg/m^3$and 16.67mpy respectively. The weight loss tests revealed low corrosion rate values for Al-Mg-Si/ESP composite, indicating a beneficial use for these materials in marine environments.

D. Result of Parametric Analysis

1. Hardness Parameter Analysis.

The model summary statistics, as given in Table 4 suggests a quadratic model. The model accuracy is predicted by the standard deviation of 0.23, PRESS of 10.81 and also, by the adjusted R-square of 0.9748 and predicted R-square of 0.8086. It is not aliased and has significant terms. The ANOVA of Table 5 confirms the significance of the model and its capability for accurate prediction of *Hi* within the selected limits. The significant model terms as predicted are A, B, AB, A^2, B^2. These are the only good predictors of *Hi.* For the linear terms, B has more dominant influence on H*i* then A. For the square terms A^2 has more dominant influence on H*i* than B^2. As shown in Table 6, the predicted R-square was found to be in reasonable agreement with the adjusted R-square value since the difference is less than 0.2. The adequacy precision of 62.861 is greater than 4 and therefore a desirable signal to noise ratio. This indicates that there is adequate signal, and that this model can be used to navigate the design space. The models for the hardness response (*Hi*), given in terms of the coded and actual factors A and B respectively are as follows:

$$H(A, B) = 31.28 + 0.72\,A - 1.47B + 1.82\,AB + 2.86A^2 - 1.89B^2 \text{----------(4.1)}$$

$$H(A, B) = 43.95758 - 0.57479A + 2.44697B + 0.073AB + 0.00457455\,A^2 - 1.89091\,B^2 \text{--(4.2)}$$

TABLE 4: MODEL SUMMARY STATISTICS

Source	Std. Dev.	R-Squared	Adjusted R-Squared	Predicted R-Squared	PRESS	
Linear	1.30	0.2832	0.2234	-0.3982	78.95	
2FI	1.09	0.5191	0.4564	-0.0431	58.90	
Quadratic	0.23	0.9796	0.9748	0.8086	10.81	Suggested
Cubic	0.075	0.9981	0.9974	0.8007	11.25	Aliased

TABLE 5: ANOVA FOR RESPONSE SURFACE QUADRATIC MODEL OF HARDNESS

Source	Sum of Squares	Df	Mean Square	F Value	p-value Prob> F	
Model	55.31	5	11.06	202.07	< 0.0001	Significant
A-ESP Size	*3.08*	*1*	*3.08*	*56.29*	*< 0.0001*	
B-ESP Con	*12.91*	*1*	*12.91*	*235.76*	*< 0.0001*	
AB	*13.32*	*1*	*13.32*	*243.36*	*< 0.0001*	
A^2	*25.69*	*1*	*25.69*	*469.29*	*< 0.0001*	
B^2	*11.24*	*1*	*11.24*	*205.27*	*< 0.0001*	
Residual	1.15	21	0.055			
Lack of Fit	*1.15*	*3*	*0.38*			
Pure Error	*0.000*	*18*	*0.000*			
Cor Total	56.46	26				

TABLE 6: QUADRATIC MODEL STATISTICS

Std. Dev.	0.23		R-Squared	0.9796
Mean	31.50		Adj R-Squared	0.9748
C.V. %	0.74		Pred R-Squared	0.8086
PRESS	10.81		Adeq Precision	62.861

Figure 5 reveals the predicted *Hi* to have nonlinear relationship with both factors A and B and that the influence of these factors on *Hi* is equally significant at both lower and higher levels. *Hi* is much more at low level of 'B' and high level of A. *Hi* initially increased before decreasing with increase in 'B' beyond the reference point at high level input. On the other hand, *Hi* is much less at low than at high levels of 'A'. It decreased with increase in 'A' to the reference point and then increased from the same point to the highest value. The implication of this behavior is that hardness values are maximized when both factors are set at the reference points. These behaviors can also be seen in the contour and response surface plots given in Figures 6 and 7.

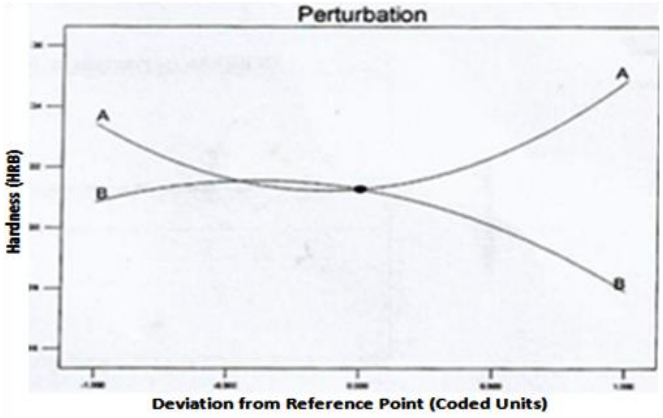

Figure 5: A Plot of *Hi* against the Perturbation

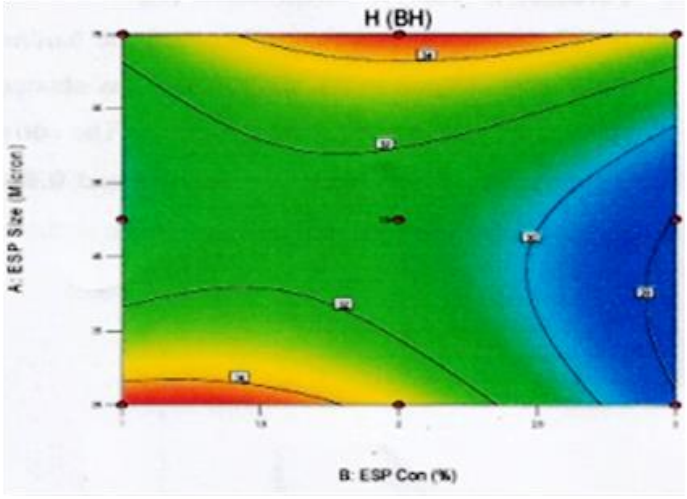

Figure 6 A Contour plot of *Hi* against A and B

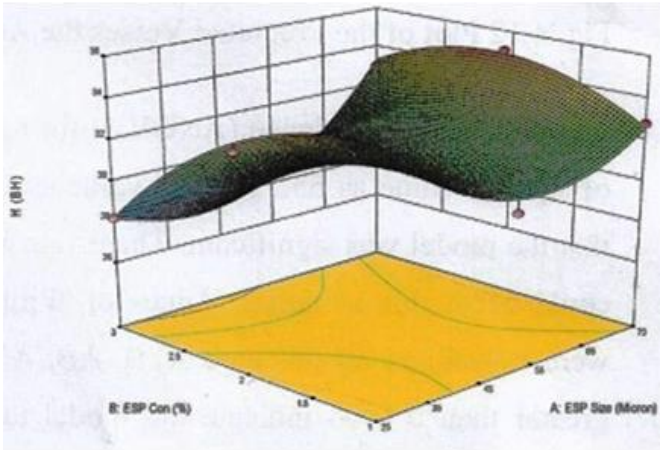

Figure 7 A Response Surface Plot of *Hi* against A and B

2. Yield Strength Parameter Analysis.

Table 7 is the model summary statistics for the yield strength data. It shows a quadratic regression model is adequate and accurate fit for the response data. It recorded a standard deviation of 8.447E-003, R-squared value of 0.9902, adjusted R-squared value of 0.9879, and predicted R-squared value of 0.9311. Table 8 is analysis of variance (ANOVA). It showed the model is significant for accurate prediction of the yield strength (YS) within the design limits of factors A and B. It also showed that the model terms A, B, AB and A^2 only are significant. For the linear terms, 'A' has dominant influence on *YSi* than 'B'. For the square terms, A^2 has dominant influence than B^2. Table 9 is the quadratic model statistics. It reveals the predicted R-squared value of 0.9311 to be in reasonable agreement with the adjusted R-squared value of 0.9879, since the difference is less than 0.2. The adequacy precision of 68.926, greater than 4, is a desirable signal to noise ratio. This indicates that there is adequate signal, and that this model can also be used to

navigate the design space. The models for the yield strength (YS) given in terms of the coded and actual factors A, and B are as follows:

$$Log_{10}YS(A,B) = 1.47 - 0.01A - 0.011B - 0.11AB + 0.14A^2 + 0.005225B^2 \quad (4.3)$$

$$Log_{10}YS(A,B) = 1.69066 - 001.5031A + 0.18760B - 0.00438771AB + 0.0002296A^2 + 0.00522535B^2 \quad (4.4)$$

TABLE 7: MODEL SUMMARY STATISTICS

Source	Std. Dev.	R-Squared	Adjusted R-Squared	Predicted R-Squared	PRESS	
Linear	0.079	0.0224	-0.0591	-1.0478	0.31	
2FI	0.066	0.3365	0.2499	-1.5820	0.40	
Quadratic	8.447E-003	0.9902	0.9879	0.9311	0.011	Suggested
Cubic	8.788E-003	0.9904	0.9869	0.0017	0.15	Aliased

TABLE 8: ANOVA FOR RESPONSE SURFACE QUADRATIC MODEL OF THE YIELD STRENGTH

Source	Sum of Squares	df	Mean Square	F Value	p-value Prob> F	
Model	0.15	5	0.030	425.37	< 0.0001	significant
A-ESP Size	*2.719E-003*	*1*	*2.719E-003*	*38.11*	*< 0.0001*	
B-ESP Con	*7.110E-004*	*1*	*7.110E-004*	*9.97*	*0.0048*	
AB	*0.048*	*1*	*0.048*	*674.61*	*< 0.0001*	
A^2	*0.065*	*1*	*0.065*	*906.71*	*< 0.0001*	
B^2	*8.581E-005*	*1*	*8.581E-005*	*1.20*	*0.2852*	
Residual	1.498E-003	21	7.135E-005			
Lack of Fit	*1.498E-003*	*3*	*4.994E-004*			
Pure Error	*0.000*	*18*	*0.000*			
Cor Total	0.15	26				

TABLE 9: QUADRATIC MODEL STATISTICS

Std. Dev.	8.447E-003	R-Squared	0.9902
Mean	1.50	Adj R-Squared	0.9879
C.V. %	0.56	Pred R-Squared	0.9311
PRESS	0.011	Adeq Precision	68.926

Figure 8 shows *YS* to have a nonlinear relationship with factor 'A' but linear with 'B'. It is important to note that *YSi* decreased slightly with increase in B but maintained high values at low factor levels. More specifically, *YSi* is much more at low levels of 'A' and 'B'. It decreased with increase in 'A' to the reference point and then increased from the same point to a higher value. These behaviors have implication of *YSi* being maximized when the factors A and B are set at the mid-level of their values. This can be seen in the contour and response surface plots given in Figures 9 and 10 respectively where the factors were observed interacting with each other.

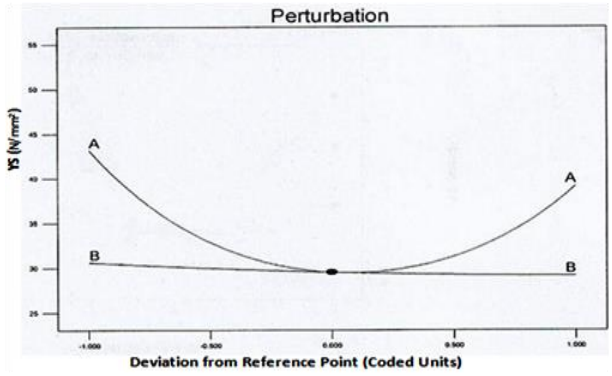

Figure 8 A Plot of *YSi* against the Perturbation

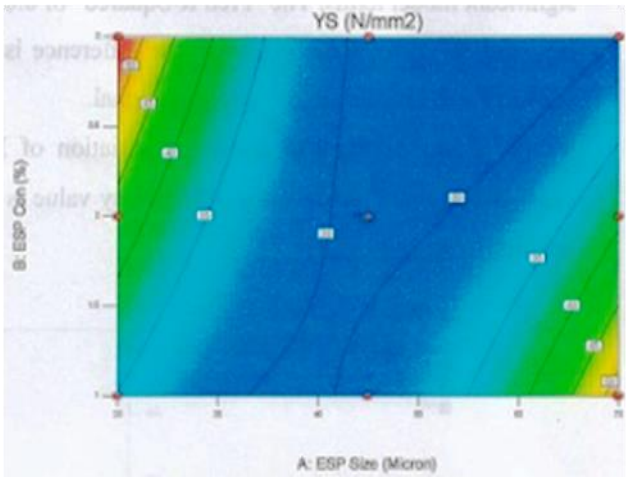

Figure 9: A Contour plot of *YS* against A and

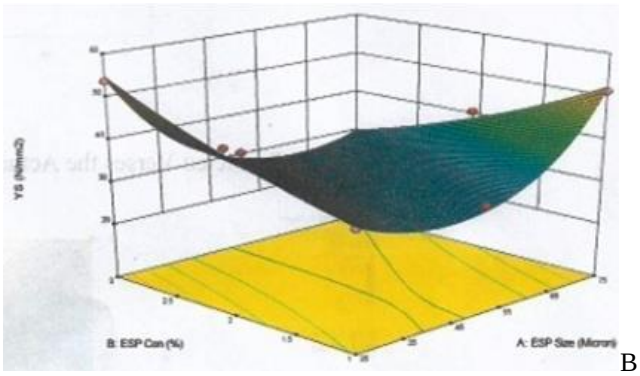

B

Figure 10 A Response Surface plot of *YSi* against Aand B

3. Modulus of Elasticity Parameter Analysis.

Shown in Table 10 is the model summary statistics that suggests a quadratic model for the analysis of modulus of elasticity (ME).The model accuracy is predicted by the standard deviation of 554.92, PRESS of 6.178E+007, the adjusted R-square of 0.9809 and also by predicted R-squared value of 0.8527. It is not aliased and has significant model terms of A, B, AB, A^2, B^2. The ANOVA of Table 11 confirms the significance of the model and its capability for accurate prediction of *MEi* within the selected limits. The model F-value of 268.22 implies the model is significant. These are all good predictors of *MEi*. For the linear terms, 'A' has more dominant influence on *MEi* then 'B'. For the square terms B^2 has more dominant influence on *MEi* than A^2. As shown in Table 12, the predicted R-square of 0.8527 was found to be in reasonable agreement with the adjusted R-square of 0.9809 since the difference is less than 0.2. The adequacy precision of 81.307 is greater than 4 and therefore a desirable signal to noise ratio. This indicates that there is adequate signal, and that this model can be used to navigate the design space. The models for the modulus of elasticity (*MEi*), given in terms of the coded and actual factors A and B respectively, are as follows:

$$ME\,(A, B) = 12061.48 + 6470.83A + 678.17B + 31091.25AB + 4907.41A^2 - 5896.59B^2 \quad \text{---------- (4.5)}$$

$$ME\,(A, B) = 6243.75758 - 775.09212A + 18046.0303B + 124.37AB + 7.85185A^2 - 896.59091B^2 \quad \text{---(4.6)}$$

TABLE 10: MODEL SUMMARY STATISTICS

Source	Std. Dev.	R-Squared	Adjusted R-Squared	Predicted R-Squared	PRESS	
Linear	2625.60	0.6055	0.5727	0.2834	3.006E+008	
2FI	2347.81	0.6977	0.6583	0.4757	2.199E+008	
Quadratic	554.92	0.9846	0.9809	0.8527	6.178E+007	Suggested
Cubic	112.01	0.9994	0.9992	0.9407	2.485E+007	Aliased

TABLE 11: ANOVA FOR RESPONSE SURFACE QUADRATIC MODEL OF MODULUS OF ELASTICITY

Source	Sum of Squares	df	Mean Square	F Value	p-value Prob> F	
Model	4.130E+008	5	8.259E+007	268.22	< 0.0001	significant
A-ESP Size	*2.512E+008*	*1*	*2.512E+008*	*815.84*	*< 0.0001*	
B-ESP Con	*2.759E+006*	*1*	*2.759E+006*	*8.96*	*0.0069*	
AB	*3.867E+007*	*1*	*3.867E+007*	*125.58*	*< 0.0001*	
A^2	*7.569E+007*	*1*	*7.569E+007*	*245.79*	*< 0.0001*	
B^2	*1.093E+008*	*1*	*1.093E+008*	*354.86*	*< 0.0001*	
Residual	6.467E+006	21	3.079E+005			
Lack of Fit	*6.467E+006*	*3*	*2.156E+006*			
Pure Error	*0.000*	*18*	*0.000*			

TABLE 12: QUADRATIC MODEL STATISTICS

Std. Dev.	554.92		R-Squared	0.9846
Mean	11841.67		Adj R-Squared	0.9809
C.V. %	4.69		Pred R-Squared	0.8527
PRESS	6.178E+007		Adeq Precision	81.307

Figure 11 shows the predicted *MEi* to have nonlinear relationship with both factors A and B. *MEi* is equally significant at both lower and higher levels. *MEi* is much more at high levels of 'A' and 'B', slightly decreased with increase in 'A' to a point before increasing beyond the reference point and then to the highest value at high level. On the other hand, *MEi* is much less at low levels of 'A' and 'B', increasing with increase in 'B' to the reference point and then decreased from the same point to a lower value at high level. The implication of this behavior is that hardness values are maximized when both factors are set at the reference points. These behaviors can also be seen in the contour and response surface plots given in Figures 12 and 13

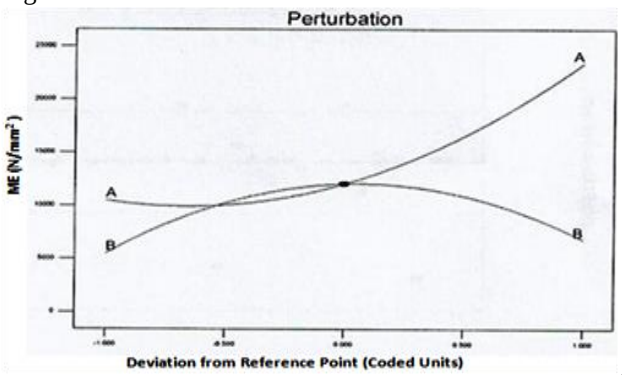

Figure 11 A Plot of *MEi* against Perturbation

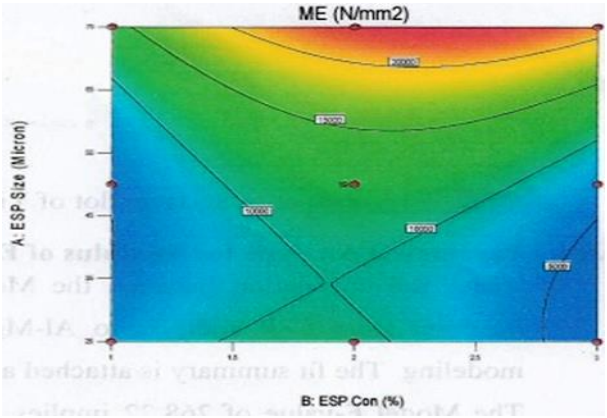

Figure 12 A Contour Plot of *MEi* against A and B

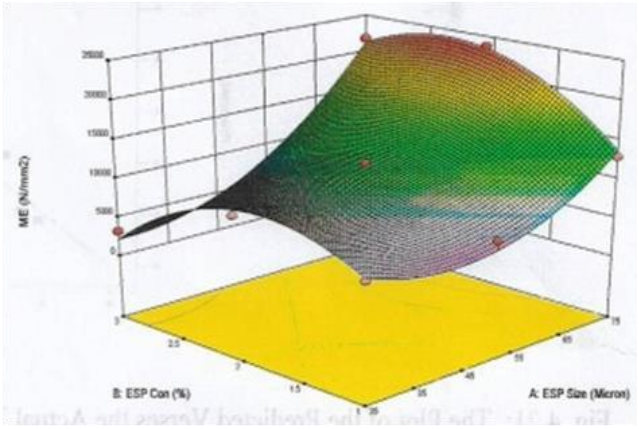

Figure 13 A Response Surface Plot of *MEi* against A and B

***4. Thermal Conductivity Parameter Analysis*.**

Table 13 is the model summary statistics for the thermal conductivity (TC) data. It shows a two factor interaction (2FI) regression model is adequate and accurate fit for the response data. It recorded a standard deviation of 2.24, R-squared value of 0.9302, adjusted R-squared value of 0.9211, and predicted R-squared value of 0.7959. Table 14 is analysis of variance (ANOVA). It shows the model is significant for accurate prediction of the thermal conductivity (TC) within the design limits of factors A and B. It also showed that the model terms A, B and AB only are significant, with 'A' having more dominant influence on *TCi* than 'B'. Table 15 is the quadratic model statistics. It reveals the predicted R-square value of 0.9302 to be in reasonable agreement with the adjusted R-square value of 0.9211, since the difference of 0.0091 is less than 0.2. The adequacy precision of 53.569, greater than 4, is a desirable signal to noise ratio. This indicates that there is adequate signal, and that this model can also be used to navigate the design space. The models for the thermal conductivity (*TCi*), given in terms of the coded and actual factors A, B and C are as follows:

$$TC\,(A, B) = 47.04 + 5.63\,A + 4.64B + 17.45AB \quad \text{..... (4.7)}$$

$$TC\,(A, B) = 96.29407 - 1.17067A - 30.25833B + 0.69800AB \quad \text{..... (4.8)}$$

TABLE 13: MODEL SUMMARY STATISTICS

Source	Std. Dev.	R-Squared	Adjusted R-Squared	Predicted R-Squared	PRESS	
Linear	7.45	0.1934	0.1262	-0.9846	3280.59	
2FI	2.24	0.9302	0.9211	0.7959	337.36	Suggested
Quadratic	2.31	0.9322	0.9161	0.5215	791.02	
Cubic	2.40	0.9339	0.9096	-5.8911	11390.89	Aliased

TABLE 14: ANOVA FOR RESPONSE SURFACE QUADRATIC MODEL OF THERMAL CONDUCTIVITY

Source	Sum of Squares	Df	Mean Square	F Value	p-value Prob> F	
Model	1537.69	3	512.56	102.24	< 0.0001	significant
A-ESP Size	*190.41*	*1*	*190.41*	*37.98*	*< 0.0001*	
B-ESP Con	*129.27*	*1*	*129.27*	*25.78*	*< 0.0001*	
AB	*1218.01*	*1*	*1218.01*	*242.95*	*< 0.0001*	
Residual	115.31	23	5.01			
Lack of Fit	*115.31*	*5*	*23.06*			
Pure Error	*0.000*	*18*	*0.000*			
Cor Total	1653.00	26				

TABLE 15: QUADRATIC MODEL STATISTICS

Std. Dev.	2.24		R-Squared	0.9302
Mean	47.04		Adj R-Squared	0.9211
C.V. %	4.76		Pred R-Squared	0.7959
PRESS	337.36		Adeq Precision	53.569

Figure 14 shows *TC* to have linear relationship with A and B. It shows the influence of both factors 'A' and 'B' on *TC* to equally of high significance. It is important to note that *TC* increased with increase in A and B. These behaviors have implication of *TC* being maximized when the factors A and B are set at the high level of their values. They can also be seen in the contour and response surface plots given in Figures 15 and 16. They can be attributed to the observed none interactions of factors.

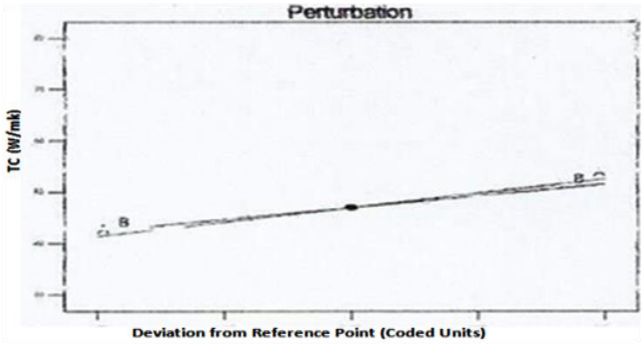

Figure 14 A Plot of *TCi against the* Perturbation

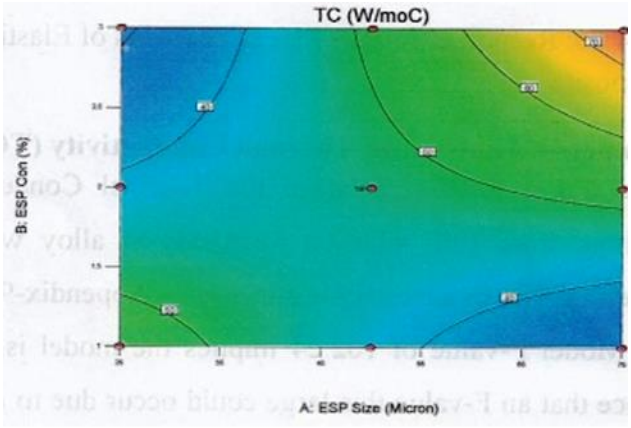

Figure 15 A Contour Plot of *TCi* against A and B

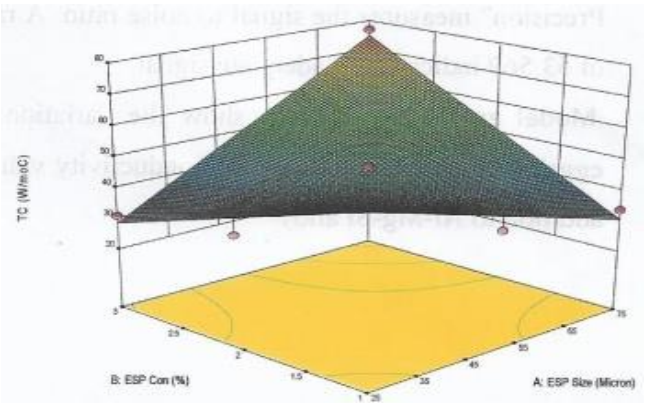

Figure 16 A Response Surface Plot of *TCi* against A and B

5. Impact Strength Parameter Analysis.

The model summary statistics, as given in Table 16, suggests a quadratic model. The model accuracy is predicted by the standard deviation of **0.46** and PRESS of 30.48 and also, by the adjusted R-square of 0.9780 and predicted R-square of 0.8753. It is not aliased and has significant terms. The ANOVA of Table 17 confirms the significance of the model and its capability for accurate prediction of *IEi* within the selected limits. The significant model terms as predicted are A, B, AB, A^2, B^2. These are the only good predictors of *IEi.* For the linear terms, B has more dominant influence on *IEi* than A. For the square terms B^2 has more dominant influence on *IEi i* than A^2. As shown in Table 18, the predicted R-square of 0.9780 was found to be in reasonable agreement with the adjusted R-square of 0.9780 since the difference is less than 0.2. The adequacy precision of 53.135 is greater than 4 and therefore a desirable signal to noise ratio. This indicates that there is adequate signal and that this model can be used to navigate the design space. The models for the impact strength (*IEi*) given in terms of the coded and actual factors A and B respectively, are as follow:

$$IE(A, B) = +20.40 - 1.29A - 2.25B - 0.50AB - 3.62A^2 - 3.74B^2 \quad \text{---------- (4.9)}$$

$$IE(A, B) = -3.95202 + 0.56712A + 13.71970B - 0.020000AB - 0.00578788A^2 - 3.74242B^2 \quad \text{----(4.10)}$$

TABLE 16: MODEL SUMMARY STATISTICS

Source	Std. Dev.	R-Squared	Adjusted R-Squared	Predicted R-Squared	PRESS	
Linear	2.92	0.1653	0.0957	-0.6336	399.21	
2FI	2.97	0.1694	0.0610	-2.6300	887.05	
Quadratic	0.46	0.9822	0.9780	0.8753	30.48	Suggested
Cubic	0.48	0.9823	0.9758	-0.8474	451.44	Aliased

TABLE 17: ANOVA FOR RESPONSE SURFACE QUADRATIC MODEL OF IMPACT ENERGY

Source	Sum of Squares	df	Mean Square	F Value	p-value Prob> F	
Model	240.01	5	48.00	231.68	< 0.0001	significant
A-ESP Size	*10.01*	*1*	*10.01*	*48.31*	*< 0.0001*	
B-ESP Con	*30.38*	*1*	*30.38*	*146.60*	*< 0.0001*	
AB	*1.00*	*1*	*1.00*	*4.83*	*0.0394*	
A^2	*41.13*	*1*	*41.13*	*198.50*	*< 0.0001*	
B^2	*44.02*	*1*	*44.02*	*212.45*	*< 0.0001*	
Residual	4.35	21	0.21			
Lack of Fit	*4.35*	*3*	*1.45*			
Pure Error	*0.000*	*18*	*0.000*			
Cor Total	244.37	26				

TABLE 18: QUADRATIC MODEL STATISTICS

Std. Dev.	0.46		R-Squared	0.9822
Mean	18.77		Adj R-Squared	0.9780
C.V. %	2.43		Pred R-Squared	0.8753

Figure 17 shows ***IEi*** to have a nonlinear relationship with both factors 'A' and 'B'. It is important to note that for both factors, ***IEi*** increased up to a point before the reference mark and then decreased to lowest values at high factor levels. More specifically, ***IEi*** is much more at low than at high levels of 'A' and 'B'. These behaviors have implication of ***IEi*** being maximized when the factors A and B are set at the low level of their values. This can be seen in the contour and response surface plots given in Figures 18 and 19 respectively, where the factors were observed interacting with each other.

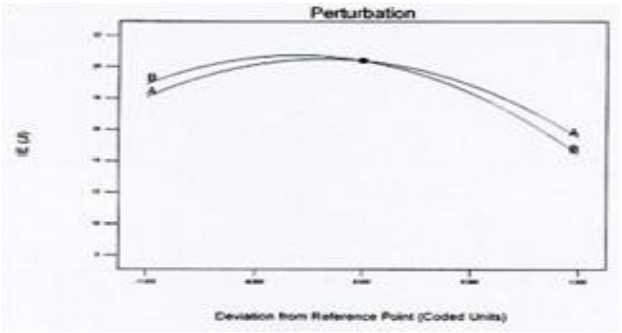

Figure 17 A Plot of *IEi* against the Perturbation

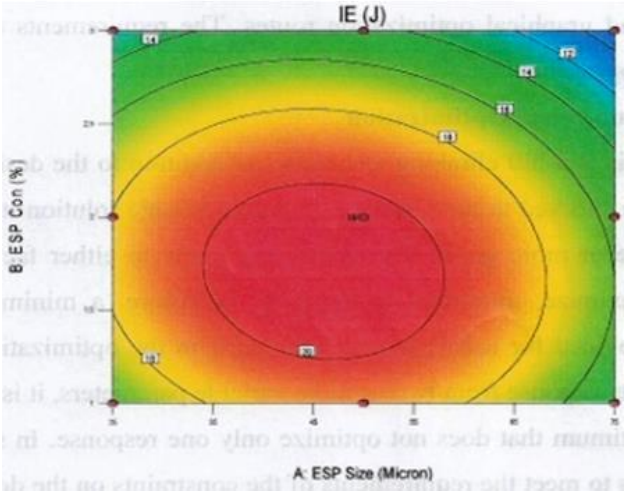

Figure 18: A Contour Plot of *IEi* against A and B

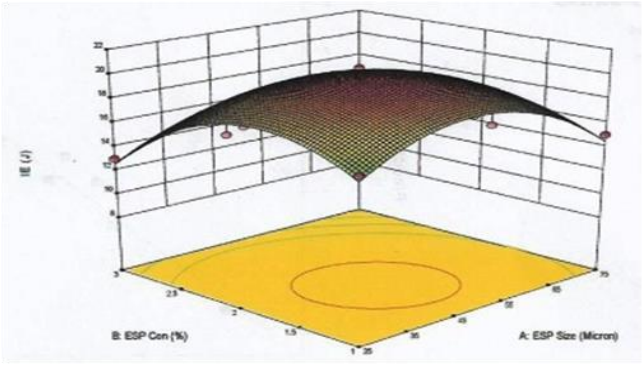

Figure 19 A Response Surface Plot of *IEi* Against A and B

6. Density Parameter Analysis.

Table 19 is the model summary statistics for the density (D) data. It shows a quadratic regression model is adequate and accurate fit for the response data. It recorded a standard deviation of 1.93, R-squared value of 0.9852, adjusted R-squared value of 0.9817, and predicted R-squared value of 0.8578. Table 20 is analysis of variance (ANOVA). It showed the model is significant for accurate prediction of the density (D) within the design limits of factors A, and B. It also showed that the model terms A, B, AB, A^2 and B^2 are significant. For the linear terms, 'B' has dominant influence on *Di* than, 'B'. For the square terms, A^2 has dominant influence than B^2. Table 21 is the quadratic model statistics. It reveals the predicted R-squared value to be in reasonable agreement with the adjusted R-squared value since the difference is less than 0.2. The adequacy precision of 74.340, greater than 4, is a desirable signal to noise ratio. This indicates that there is adequate signal, and that this model can also be used to navigate the design space. The models for the density **(D)** given in terms of the coded and actual factors A, and B are as follows

$$D(A, B) = 2595.05 + 5.50A - 15.67B - 6.25AB + 24.47A^2 + 3.97B^2 \quad \text{(4.11)}$$

$$D(A, B) = 2704.14141 - 3.19515A - 19.04545B - 0.25AB + 0.039152A^2 + 3.9697B^2 \quad \text{(4.12)}$$

TABLE 19: MODEL SUMMARY STATISTICS

Source	Std. Dev.	R-Squared	Adjusted R-Squared	Predicted R-Squared	PRESS	
Linear	12.28	0.3136	0.2564	-0.3854	7307.00	
2FI	12.27	0.3433	0.2576	-1.9355	15482.49	
Quadratic	1.93	0.9852	0.9817	0.8578	749.93	Suggested
Cubic	0.25	0.9998	0.9997	0.9763	125.05	Aliased

TABLE 20: ANOVA FOR RESPONSE SURFACE QUADRATIC MODEL OF DENSITY

Source	Sum of Squares	df	Mean Square	F Value	p-value Prob> F	
Model	5196.26	5	1039.25	279.68	< 0.0001	significant
A-ESP Size	*181.50*	*1*	*181.50*	*48.84*	*< 0.0001*	
B-ESP Con	*1472.67*	*1*	*1472.67*	*396.32*	*< 0.0001*	
AB	*156.25*	*1*	*156.25*	*42.05*	*< 0.0001*	
A^2	*1881.84*	*1*	*1881.84*	*506.44*	*< 0.0001*	
B^2	*49.53*	*1*	*49.53*	*13.33*	*0.0015*	
Residual	78.03	21	3.72			
Lack of Fit	*78.03*	*3*	*26.01*			
Pure Error	*0.000*	*18*	*0.000*			
Cor Total	5274.30	26				

TABLE 21: QUADRATIC MODEL STATISTICS

Std. Dev.	1.93		R-Squared	0.9852
Mean	2601.37		Adj R-Squared	0.9817
C.V. %	0.074		Pred R-Squared	0.8578
PRESS	749.93		Adeq Precision	74.340

Figure 20 shows *Di* to have a nonlinear relationship with factor 'A' but slightly linear with 'B'. It is important to note that *Di* decreased with increase in 'A' up to the reference point before increasing to highest value at high factor level. On the other hand, *Di* value decreased with increasing 'B' factor input from low to high level. The implication is that 'B' has more influence on *Di* values than 'A'. These behaviors have implication of *Di* being minimized when the factors A and B are set at the reference point (mid-level) of their values. This can be seen in thecontour and response surface plots given in Figures 21 and 22 where the factors were observed interacting with each other.

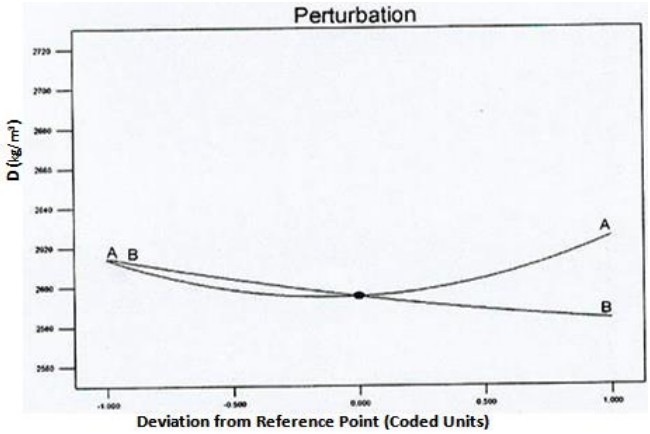

Figure 20 A Plot of *Di* against the Perturbation

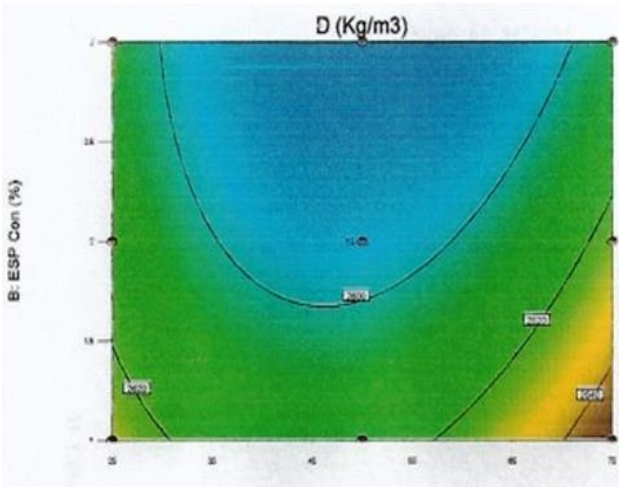

Figure 21 A Contour Plot of *Di* against A and B

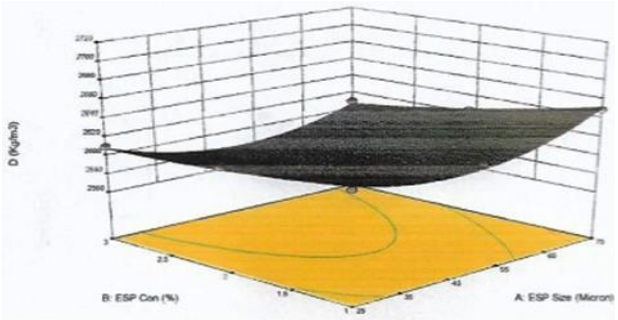

Figure 22 A Response Surface Plot of *Di* against A and B

7. Corrosion Rate Parameter Analysis.

From the model summary statistics, given in Table 22, a quadratic model is suggested to be more accurate as predicted by the least of the standard deviation of 0.52, PRESS of 41.26, the highest of the adjusted R-square of 0.9620 and predicted R-square of 0.7780.These results suggest that the model terms are significant, and that the model is not aliased. The ANOVA for response surface quadratic model of corrosion rate, given in Table 23, confirms the significance of the model as being capable of accurate prediction of *CRi* within the selected limits and also, that the model terms A, B, AB, A^2, B^2 are significant and predictors of *CRi* . The predicted R-square of 0.7780, given in Table 24, is found to be in reasonable agreement with the adjusted R-square of 0.9620 since the difference is less than 0.2. The adequacy precision of 45.373, greater than 4, is a desirable signal to noise ratio indicating that there is adequate signal, and that this model can be used to navigate the design space. The response surface models of the corrosion rate (*CRi)* given in terms of the coded factors (Equation 4.3), and also, in terms of the actual factors A and B, respectively, are:

$$CR(A, B) = 0.10 - 0.67A - 3.18B + 2.28AB + 1.54A^2 + 3.48B^2 \quad \text{---------- (4.13)}$$

$$CR(A, B) = 36.98154 - 0.45535A - 21.4147B + 0.091AB + 0.00246519A^2 + 3.47774B^2 \quad \text{----- (4.14)}$$

TABLE 22: MODEL SUMMARY STATISTICS

Source	Std. Dev.	R-Squared	Adjusted R-Squared	Predicted R-Squared	PRESS	
Linear	2.26	0.3410	0.2861	-0.3054	242.67	
2FI	2.10	0.4524	0.3810	-1.1303	396.01	
Quadratic	0.52	0.9693	0.9620	0.7780	41.26	Suggested
Cubic	0.52	0.9721	0.9619	-1.9037	539.78	Aliased

TABLE: 23: ANOVA FOR RESPONSE SURFACE QUADRATIC MODEL OF CORROSION RATE

Source	Sum of Squares	df	Mean Square	F Value	p-value Prob> F	
Model	180.19	5	36.04	132.74	< 0.0001	Significant
A-ESP Size	*2.70*	*1*	*2.70*	*9.95*	*0.0048*	
B-ESP Con	*60.69*	*1*	*60.69*	*223.55*	*< 0.0001*	
AB	*20.70*	*1*	*20.70*	*76.25*	*< 0.0001*	
A^2	*7.46*	*1*	*7.46*	*27.48*	*< 0.0001*	
B^2	*38.01*	*1*	*38.01*	*140.01*	*< 0.0001*	
Residual	5.70	21	0.27			
Lack of Fit	*5.70*	*3*	*1.90*			
Pure Error	*0.000*	*18*	*0.000*			
Cor Total	185.90	26				

TABLE 24: QUADRATIC MODEL STATISTICS

Std. Dev.	0.52	R-Squared	0.9693
Mean	1.22	Adj R-Squared	0.9620
C.V. %	42.70	Pred R-Squared	0.7780
PRESS	41.26	Adeq Precision	45.373

In Figure 23, *CRi* has nonlinear relationship with factors A and B, and that effect of these factors on *CRi* became more significant at the higher levels of these factors, when compared to that at lower levels. *CRi* decreased with increase in 'A' up to a mid-point where it increased towards high level input. The effect of 'B' on the value of *CRi* showed a decrease from low level B down to a reference point before an upswing towards high level of 'B. The implication of this behavior is that 'B' has more dominant influence on *Cri* which is minimized when factor A is set at high level and "B" set at reference point of their values. These behaviors can also be seen in the contour and response surface plots given in Figures 24 and 25. It can be attributed to the observed multiple interaction between factors.

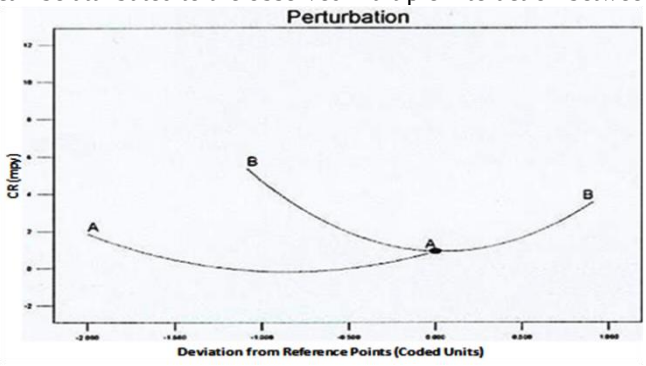

Figure 23: A Plot of *CRi* against the Perturbation

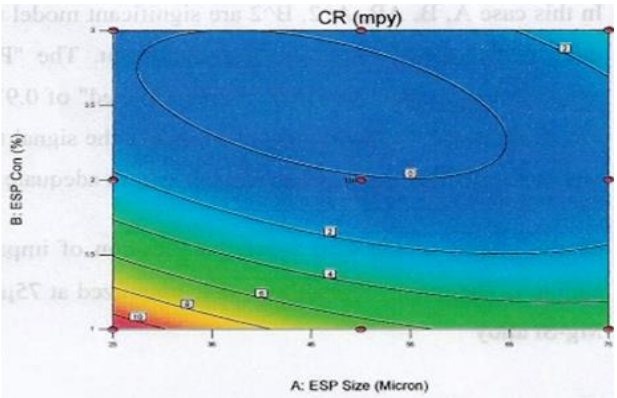

Figure 24 A Contour plot of *CRi* against A and B

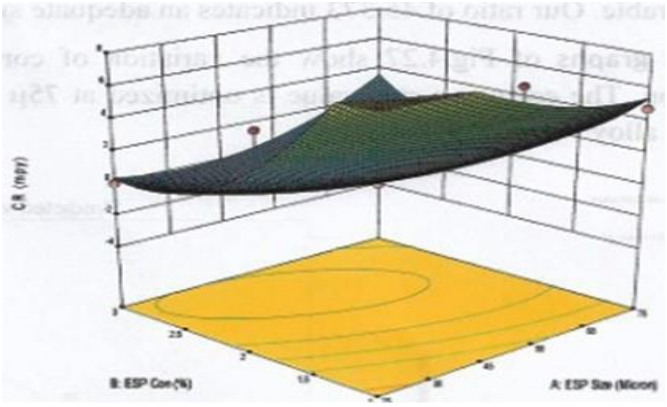

Figure 25 A Response Surface plot of *CRi* against Aand B

C. Parameter Optimization

The quality of a composite material suitable for use in engine block production depends largely on its capacity to withstand external influences such as load and environmental conditions. These performance requirements are basically determined by their hardness, yield strength, modulus of elasticity, thermal conductivity and impact strength values which are to be maximized while density and corrosion rate values are to be minimized to improve the material quality. All these were determined using appropriate standard procedures.

As given in the ramps of Figure 26, the optimum setting of the factors 'A' (ESP size) at 25 µm, and 'B' (ESP Conc.) at 1wt. %, would maximize *H* to a value of 34.876BHN, *YS* to a value of 38.163 N/mm^2, *ME* to a value of 23729.405 N/mm^2 *TC to* 54.672 W/m.^{o}C, and *IE* to 15.218 J while minimizing *D* to a value of 2623.058 Kg/m^3 and *CR* to a value of 0.921 MPY respectively with desirability of 0,940332, 0.363653, 1.00, 0.516979, 0.519945, 0.37036 and 0.916263 which occurred within the selected design space as shown by the graph of overall desirability of Figure. 4.27. The graph tells how well each variable satisfies the criteria. Values near one (1) such as modulus of elasticity (stiffness), hardness and corrosion rate are good *H*, *YS*, *ME*, *TC* and *IE* where maximized at high values of A and B while D and *CR* were minimized at high values of A and B

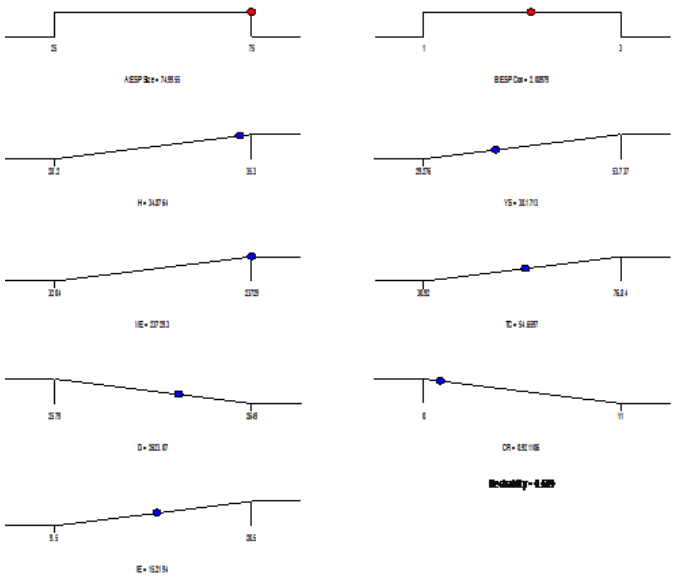

Figure 26: Optimum Setting of the Process Variables, Which Maximized Hardness, Yield Strength, Modulus of Elasticity, Thermal Conductivity and Impact Strength But Minimized Density and Corrosion Rate Values

Figure 27 Desirability Bar Plot

The optimization process yielded six (6) possible solutions as shown in Table 25. The point predicted outcome on a confidence interval of 95% is 74.99 and 2.09 ESP concentration and size respectively. The experimental run R_8 produced the optimum result and is therefore the candidate composite material developed in this study. This composite material contained Al-Mg-Si alloy with 2% wt. Concentration of 75µ sized ESP addition. The chemical composition of the developed composite is as shown in Table 26.

TABLE 25 OPTIMIZED SOLUTIONS

Solutions											
Number	ESP Size	ESP Con	H	YS	ME	TC	D	CR	IE	Desirability	
1	74.993	2.090	34.876	38.163	23729.405	54.672	2623.058	0.921	15.218	0.609	Selected
2	74.998	2.101	34.877	38.056	23761.017	54.908	2622.844	0.919	15.180	0.609	
3	25.000	1.885	33.781	42.056	10699.874	42.886	2615.158	2.991	18.230	0.525	
4	25.000	1.906	33.720	42.259	10674.320	42.613	2614.939	2.859	18.210	0.524	
5	25.068	1.867	33.817	41.811	10706.853	43.123	2615.227	3.093	18.261	0.524	
6	25.000	2.000	33.427	43.166	10498.061	41.411	2614.020	2.317	18.078	0.521	

TABLE 26 CHEMICAL COMPOSITION OF DEVELOPED COMPOSITE

Elements	Al	Si	S	Ca	Ti	Mn	Fe	Cu	Zn	Sn	Be	Pb	Bal	Total
Composition (wt.%)	69.215	1.971	0.541	0.12	0.018	0.033	0.297	0.038	0.042	0.003	0.02	0.016	27.695	99.999

IV. CONCLUSION

In this Study, aluminum composite material was formulated by reinforcing Al-Mg-Si alloy with calcined eggshell particulates using response surface methodology (RSM) in the Design Expert 9 software environment.

The castability of the composite is enhanced by the high presence of silicon which improves the fluidity of the molten composite and enables it to exhibit excellent dimensional stability, surface hardness and wear resistant properties. This is consistent with the findings of [1]. Using this material, components can be produced economically from conventional permanent molds or sand casting.

Calcined chicken eggshell can be used as particulate reinforcement of Al-Mg-Si alloy to tremendously enhance the quality and functionality of the blend to satisfy key application requirements of hardness, yield strength, elasticity, thermal conductivity and impact strength values with reduced weight and improved corrosion resistance. Eggshell particulate addition in this study improved the hardness, yield strength, elasticity and thermal conductivity values of the alloy from 30 to 33.7 HRB, 42.235 to 44.838 N/mm^2, 7,208 to 23,728 N/mm^2 and 83.88 to 95.28 W/mk respectively. Weight decreased from 2748 to 2624 Kg/m^3. However, there was a drop in impact strength from 25 to 13.5 Joules. According to [30], it is therefore an ideal low cost aluminum alloy composite suitable for applications in the temperature range of between 260^{o}c to about 400^{o}c such as motorcycle aluminum engine block..

REFERENCE

[1] A.J. Lee, "Cast Aluminum Alloy for High Temperature Applications", *The Minerals, Metals & Materials Society, NASA-Marshall Space Flight Center,* Mail Code ED33, Huntsville, AL 35812, USA, 2003

[2] P. Ramona, R Gunther, B. Josef, A. Helmut, J.U. Peter, and P. Stefan, "Property Criteria for Automotive Al-Mg-Si Sheet Alloys", [online] by *Multi-disciplinary Digital Publishing Institute* (MDPI) doi: 10.3390/ma7075047, 2014.

[3] Aalco Metals Limited,. Registered in England & Wales 3551533. VAT No. 711115591, 2015.

[4] B.O. Adewuyi and J.A. Omotoyinbo, "Effects Of Cooling Media on The Mechanical Properties and Microstructure of Sand and Die Casting Aluminium Alloys". *Journal of Science and Technology.* 28 (1), 97–102, 2008.

[5] J.O. Agunsoye, S.A. Bello, I. S. Talabi, A.A. Yekinni, I.A. Raheem, A.D Oderinde and T.E Idegbekwu, "Recycled Aluminium Cans/Eggshell Composites: Evaluation of Mechanical and Wear Resistance Properties", *Tribology in Industry* Vol. 37, No. 1 (2015)107-116, 2015.

[6] **S. A.** Bello, A. R. Isiaka and K.. R. Nasir, "Study Of Tensile Properties, Fractography and Morphology of Aluminium(1xxx)/Coconut Shell Micro Particle Composites". *Journal of King Saud University – Eng. Sciences,* http://dx.doi.org/10.1016/j.jksues.2015.10.001.

[7] G. Phil and M. Zhihong, "High Value Products from Hatchery Waste", RIRDC publication no .09/061. glatz.phil@saugov.sa.gov.au, 2009.

[8] S. B. Hassan and V.S. Aigbodion,, "Effects Of Eggshell On the Microstructures And Properties of Al–Cu–Mg/Eggshell Composites" .*Journal of King Saud University. of Engineering Science* Vol. 27, Pg 49–56, 2015.

[9] A.K. Iyer and J.M. Torkelson, "Green Composites of Polypropylene And Eggshell:Effective Biofiller Size Reduction And Dispersion By Single-Step Processing With Solid-State Shear Pulverization", *Elsevier Ltd Composites Science and Technology* 102 152–160, 014.

[10] M.C. Yew, N.H. Ramli-Sulong, M.K.. Yew, M.A. Amalina and M.R Johan, "The Formulation And Study of The Thermal Stability And Mechanical Properties of An Acrylic Coating Using Chicken Eggshell As A Novel Bio-Filler", *Elsevier B.V, Progress in Organic Coatings* 76 1549–1555, 2013.

[11] J. Senthil and P. Madan-Raj, "Preparation and Characterization of Reinforced Eggshell Polymer Composites." *International Journal on Mechanical Engineering and Robotics (IJMER).* ISSN [Print] 2321-5747, Volume-3, Issue-3, 2015.

[12] R. M. Mohammed and N. H. Ahmed, "Effect of Eggshells Powder on Some Mechanical and Physical Properties Of Natural Rubber (NR)", *The Iraqi Journal For Mechanical And Material Engineering,* Vol.12, No.3, 2012.

[13] S.C. Nwanonenyi and C.O. Chike–Onyegbula, "Water Absorption, Flammability and Mechanical Properties of Linear Low Density Polyethylene/Egg Shell Composite", *Academic Research International*, ISSN-l: 2223-9553, ISSN 2223-9944 vol. 4, 2013.

[14] H. M. Hussien, "Studying the Ultrasonic Properties, DC Conductivity and Coefficient of Thermal Conductivity of PVA-Egg Shells Composites" *Advances in Physics Theories and Applications* www.iiste.org ISSN 2224-719X [Paper] ISSN 2225-0638 [Online] Vol.18, 2013.

[15] H. J. Widad, "Comparison Study of Hardness, Thermal Conductivity and Electrical Properties of White and Brown Chiken Eggshells". *Advances in Physics Theories and Application.* ISSN 2224-719X (Paper) ISSN 2225-0638 (Online), vol 44, 2015.

[16] N. Kumar and N. Uppal, "A Review on Various Optimization Techniques used in Turning Operation for Improving Surface Roughness", *Mechanical Confab,* Vol. 2, No. 4, 45 -51, 2013.

[17] A. Aggarwal and H. Singh, "Optimization of Machining Techniques–A Retrospective and Literature Review", *Sadhana,* Vol. 30, Part 6, 699 – 711, 2005.

[18] C.O. Izelu, S.C. Eze and D.K Garba, "A Study on the Effect of Depth of Cut, Feed Rate and Tool Overhang on the Induced Vibration and Surface Roughness During Hard Turning of 41Cr4 Alloy Steel Using Response Surface Methodology", *Inter. Journal of Emerging Technology and Advanced Engineering* , Vol. 6, Issue 3 pg 54-68, 2016.

[19] C.O. Izelu and S.C. Eze, "An Investigation on Influence of Depth of Cut, Feed Rate and Work-Piece Overhang on Induced Vibration and Surface Roughness During Hard Turning of 41Cr4 Alloy Steel Using Response Surface Methodology", *International Journal of Innovative Research in Science, Engineering and Technology,* Vol. 5, Issue 3 pg 4428-4440, 2016.

[20] S. K. Gauri and S. Chakraborty, "Optimization of Multiple Responses for WEDM Processes Using Weighted Principal Components". *The International Journal of Advanced Mfrg Technology,* 40(11-12), 1102-1110, 2009.

[21] B. Deng, Y. Shi, T. Yu, C. Kang and P. Zhao, "Multi-Response Parameter Interval Sensitivity and Optimization for the Composite Tape Winding Process", Materials MDPI, doi: 10.3390/ma11020220 PMCID, 2018.

[22] P. Saini, S. Parkash and D. Choudhary, "Experimental Investigation of Machining Parameters for Surface Roughness in High Speed CNC Turning of EN-24 Alloy Steel using Response Surface Methodology", *International Journal of Engineering Research and Applications*, Vol. 4,Issue 5 153 – 160, 2014.

[23] S .Rajakumar and V. Balasubramanian, "Multi-Response Optimization of Friction-Stir-Welded AA1100 Aluminum Alloy Joints". *Journal of Mat. Engineering and Performance*. 2011.

[24] L.B Abhang and M. Hameedullah, "Optimization of Power Consumption by Desirability Function Approach", *International Journal on Resent Trends in Engineering and Technology.* Vol. 6, No. 2 pages 287 – 290, 2011.

[25] D. Vijayan and V. Seshagiri Rao, "Parametric Optimization of Friction Stir Welding Process of Age Hardenable Aluminum Alloys−ANFIS Modeling". *Journal of Central South University*. 23(8):1847-57, 2016.

[26] J. Bienia, M. Walczak, B. Surowska and J. Sobczaak, **"**Microstructure And Corrosion Behaviour Of Aluminum Fly Ash Composites", *Journal of Optoelectronics and Advanced Materials* Vol. 5, No. 2, p. 493 – 502, 2003.
[27] B.N. Mohammad and P.P. Akpan, "Behavior of Aluminum Alloy Castings Different Pouring Temperatures and Speeds", http://lejpt.academicdirect.org/A11/071. 2006.
[28] P. Sahoo, "Optimization of Turning Parameters for Surface Roughness Using RSM and GA", *Advances in Production Engineering and Management*, Vol. 6, No. 3 pages 197 – 208 2011.
[29] M. Zamani, "Al-Si Cast Alloys-Microstructure and Mechanical Properties at Ambient and Elevated Temperature**"** *School of Engineering, Jönköping University, Department of Materials and Manufacturing* SE-551 11 Jönköping, Sweden, 2016..
[30] S. Cheng, G. Yang, Z. Man, J. Wang and Y. Zhou, "Mechanical Properties And Fracture Mechanisms of Aluminum Matrix Composites Reinforced By Al_9(Co, **Ni)**$_2$ Inter-metallics" *Transactions of Nonferrous Metals Society of China* Vol. 20, Issue 4, Pages 572-576. 2010.